

## ORIGINAL ARTICLE



# Single-Molecule Localization of the Cardiac Voltage-Gated Sodium Channel Reveals Different Modes of Reorganization at Cardiomyocyte Membrane Domains

Sarah H. Vermij<sup>1</sup>, PhD; Jean-Sébastien Rougier, PhD; Esperanza Agulló-Pascual<sup>2</sup>, PhD; Eli Rothenberg<sup>3</sup>, PhD; Mario Delmar<sup>4</sup>, MD, PhD; Hugues Abriel<sup>1</sup>, MD, PhD

**BACKGROUND:** Mutations in the gene encoding the cardiac voltage-gated sodium channel  $Na_v1.5$  cause various cardiac arrhythmias. This variety may arise from different determinants of  $Na_v1.5$  expression between cardiomyocyte domains. At the lateral membrane and T-tubules,  $Na_v1.5$  localization and function remain insufficiently characterized.

**METHODS:** We used novel single-molecule localization microscopy and computational modeling to define nanoscale features of  $Na_v1.5$  localization and distribution at the lateral membrane, the lateral membrane groove, and T-tubules in cardiomyocytes from wild-type (N=3), dystrophin-deficient (*mdx*; N=3) mice, and mice expressing C-terminally truncated  $Na_v1.5$  ( $\Delta$ SIV; N=3). We moreover assessed T-tubules sodium current by recording whole-cell sodium currents in control (N=5) and detubulated (N=5) wild-type cardiomyocytes.

**RESULTS:** We show that  $Na_v1.5$  organizes as distinct clusters in the groove and T-tubules which density, distribution, and organization partially depend on SIV and dystrophin. We found that overall reduction in  $Na_v1.5$  expression in *mdx* and  $\Delta$ SIV cells results in a nonuniform redistribution with  $Na_v1.5$  being specifically reduced at the groove of  $\Delta$ SIV and increased in T-tubules of *mdx* cardiomyocytes. A T-tubules sodium current could, however, not be demonstrated.

**CONCLUSIONS:**  $Na_v1.5$  mutations may site-specifically affect  $Na_v1.5$  localization and distribution at the lateral membrane and T-tubules, depending on site-specific interacting proteins. Future research efforts should elucidate the functional consequences of this redistribution.

**GRAPHIC ABSTRACT:** A graphic abstract is available for this article.

**Key Words:** cardiac arrhythmias ■ cardiomyocyte ■ dystrophin ■ electrophysiology ■ membranes ■ microscopy ■ sodium channel

Proper function of the heart greatly depends on the cardiac voltage-gated sodium channel  $Na_v1.5$ .  $Na_v1.5$  generates the rapid upstroke of the cardiac action potential; thus, it is pivotal for cardiac excitability.<sup>1,2</sup> Mutations in its gene *SCN5A* have been associated with many cardiac arrhythmias, including Brugada

syndrome.<sup>3</sup> This diversity in cardiac arrhythmias remains unexplained. The key may lie in the distribution of  $Na_v1.5$  over specific membrane domains—pools—of the cardiomyocyte.  $Na_v1.5$  pools are regulated by different proteins, so a given *SCN5A* mutation may disturb the interaction with a specific protein and affect a specific pool.  $Na_v1.5$

Correspondence to: Prof Hugues Abriel, MD, PhD, Institute of Biochemistry and Molecular Medicine, University of Bern, Bühlstrasse 28, 3012 Bern, Switzerland. Email [hugues.abriel@ibmm.unibe.ch](mailto:hugues.abriel@ibmm.unibe.ch)

The Data Supplement is available at <https://www.ahajournals.org/doi/suppl/10.1161/CIRCEP.119.008241>.

For Sources of Funding and Disclosures, see page 638.

© 2020 The Authors. *Circulation: Arrhythmia and Electrophysiology* is published on behalf of the American Heart Association, Inc., by Wolters Kluwer Health, Inc. This is an open access article under the terms of the [Creative Commons Attribution Non-Commercial-NoDerivs](https://creativecommons.org/licenses/by-nc-nd/4.0/) License, which permits use, distribution, and reproduction in any medium, provided that the original work is properly cited, the use is noncommercial, and no modifications or adaptations are made.

*Circulation: Arrhythmia and Electrophysiology* is available at [www.ahajournals.org/journal/circep](http://www.ahajournals.org/journal/circep)

### WHAT IS KNOWN?

- The cardiac voltage-gated sodium channel Na<sub>v</sub>1.5 is expressed at different cardiomyocyte membrane domains where it interacts with domain-specific proteins.
- Due to heart failure or genetic variants, Na<sub>v</sub>1.5 localization patterns can change, potentially with arrhythmogenic effects.
- For several main cardiomyocyte domains, these effects have only been investigated with diffraction-limited microscopy methods.

### WHAT THE STUDY ADDS?

- Using single-molecule localization microscopy, we define nanoscale features of Na<sub>v</sub>1.5 localization and distribution at the lateral membrane and the T-tubules.
- We demonstrate redistribution of Na<sub>v</sub>1.5 at the lateral and T-tubular membranes of cardiomyocytes from dystrophin-deficient mice and mice expressing C-terminally truncated Na<sub>v</sub>1.5 (ΔSIV).
- This study indicates the importance of nanoscale characterization of wild-type and mutated Na<sub>v</sub>1.5 and its regulators.

### Nonstandard Abbreviations and Acronyms

<b>Bin1</b>	bridging integrator 1
<b>CASK</b>	calcium/calmodulin-dependent serine protein kinase
<b>IF</b>	interaction factor
<b><i>I</i><sub>Na</sub></b>	sodium current
<b><i>mdx</i></b>	dystrophin-deficient mouse model
<b>Na<sub>v</sub>1.5</b>	cardiac voltage-gated sodium channel
<b>SMLM</b>	single-molecule localization microscopy
<b>WT</b>	wild type
<b>ΔSIV</b>	C-terminal Na <sub>v</sub> 1.5 serine-isoleucine-valine truncation

expression at the intercalated disc<sup>4</sup> and at the lateral membrane<sup>5</sup> is well established (Figure 1) while a third pool at the T-tubules is still disputed.<sup>6</sup> At the intercalated disc, coupling neighboring cardiomyocytes, Na<sub>v</sub>1.5 interacts with connexin-43 and N-cadherin, among others.<sup>4</sup> At the lateral membrane, Na<sub>v</sub>1.5 interacts with the syntrophin/dystrophin complex and CASK (calcium/calmodulin-dependent serine protein kinase), among others.<sup>7–9</sup> The lateral membrane is shaped distinctly with grooves and crests,<sup>10</sup> and Na<sub>v</sub>1.5 is expressed at both locations in murine cardiomyocytes (Figure 1A).<sup>11,12</sup> T-tubules are invaginations of the lateral membrane and originate in the groove. They provide a large surface for calcium handling<sup>6</sup>; consequently, the majority of the voltage-gated calcium channels is expressed at the T-tubules.<sup>13,14</sup> The

claim of a T-tubular Na<sub>v</sub>1.5 pool has so far only been supported by inconclusive results. By comparing whole-cell sodium current (*I*<sub>Na</sub>) densities in detubulated and control cardiomyocytes, T-tubular sodium channels were determined to conduct 30% of total *I*<sub>Na</sub>.<sup>15</sup> This is probably a considerable overestimation as this method relies on membrane capacitance as a measure for cell membrane area but underestimates the surface area of cardiomyocytes by ≈50%.<sup>16</sup> Therefore, the presence of a T-tubular Na<sub>v</sub>1.5 pool remains undetermined.

Our current state of knowledge regarding the localization and distribution of Na<sub>v</sub>1.5 at the lateral membrane and T-tubules is based on standard microscopy methods that are limited in resolution and sensitivity. At the T-tubules, previously published immunofluorescence data on Na<sub>v</sub>1.5 show an intracellular striated pattern for Na<sub>v</sub>1.5, but without a T-tubular marker, this pattern cannot be attributed to the T-tubules.<sup>17,18</sup> The respective confocal microscopy techniques lacked resolution to resolve the narrow T-tubular structure.<sup>17,18</sup> At the lateral membrane, cell-attached and scanning ion conductance microscopy recordings of the *I*<sub>Na</sub> have provided information on the number of functional channels in a given area at the lateral membrane or at the crest and groove<sup>11,12,19–21</sup> but did not provide the molecular features needed to characterize Na<sub>v</sub>1.5 organization at these domains. Moreover, previous studies did not correlate Na<sub>v</sub>1.5 with structural markers such as α-actinin for the groove and Bin1 (bridging integrator 1) for the T-tubules.<sup>17,18,22</sup> As such, current models of the roles of Na<sub>v</sub>1.5 at the lateral membrane and T-tubules do not represent the true molecular nature of Na<sub>v</sub>1.5 expression and organization at these domains. To address these issues, we use multicolor single-molecule localization microscopy (SMLM),<sup>23</sup> a super-resolution imaging method, providing the features of Na<sub>v</sub>1.5 organization and related markers with nanoscale resolution. We addressed Na<sub>v</sub>1.5 expression and cluster organization at the T-tubules using Bin1,<sup>24</sup> and Na<sub>v</sub>1.5 affinity for the groove using α-actinin in isolated cardiomyocytes. We assessed T-tubular *I*<sub>Na</sub> by comparing whole-cell *I*<sub>Na</sub> from control and detubulated cardiomyocytes. We then addressed the consequences of dystrophin deficiency (*mdx*) and C-terminal Na<sub>v</sub>1.5 serine-isoleucine-valine truncation (ΔSIV) on Na<sub>v</sub>1.5 expression and organization at the lateral membrane overall, at the groove, and at the T-tubules. ΔSIV resembles the p.V2016M mutation found in a Brugada syndrome patient, replacing the C-terminal valine with a methionine, which results in reduced Na<sub>v</sub>1.5 expression.<sup>5</sup> ΔSIV knockin mice display a loss of *I*<sub>Na</sub> and Na<sub>v</sub>1.5 expression specifically at the lateral membrane,<sup>5</sup> while interaction of Na<sub>v</sub>1.5-ΔSIV with the syntrophin/dystrophin complex is impaired.<sup>5</sup> *mdx* mice display a strong reduction of *I*<sub>Na</sub> and Na<sub>v</sub>1.5 expression overall and specifically at the lateral membrane.<sup>7,8</sup>

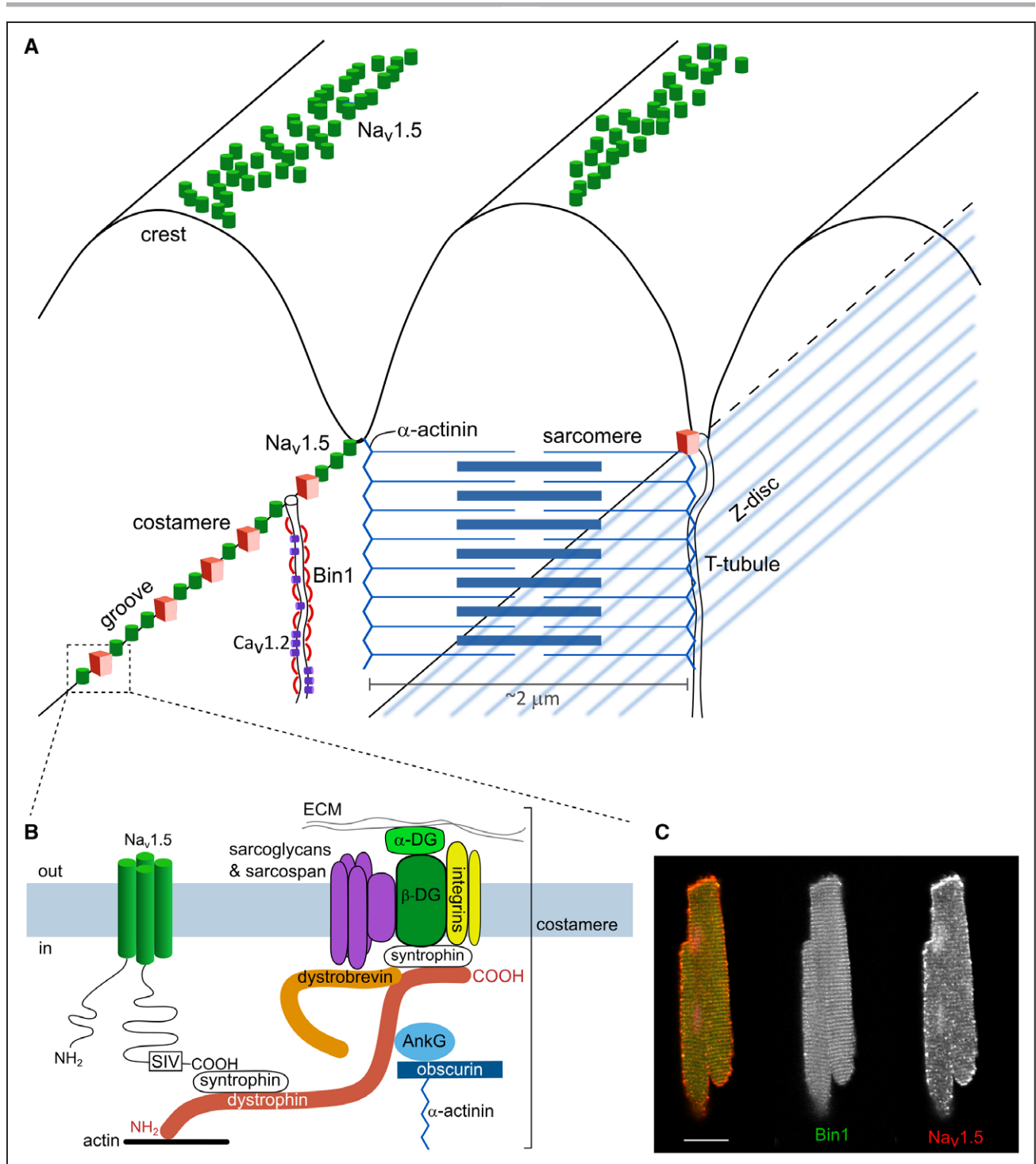


**Figure 1. Pools of the cardiac voltage-gated sodium channel Na<sub>v</sub>1.5 in the cardiomyocyte.**

**A**, The lateral membrane has a characteristic profile: at the groove, the membrane is anchored to the Z-line ( $\alpha$ -actinin; blue) through costameres (red boxes). T-tubules follow Z-lines and open to the groove. Their membrane is shaped by Bin1 (bridging integrator 1; red curves) and contain, among many other proteins, voltage-gated calcium channels (Ca<sub>v</sub>1.2; purple). Na<sub>v</sub>1.5 is expressed at the crest and the groove.

**B**, Na<sub>v</sub>1.5 (green; left) associates with the costamere (right). The SIV motif of Na<sub>v</sub>1.5 binds syntrophin (white), which binds dystrophin (red). Dystrophin also binds syntrophin associated with the costamere, which contains multiple transmembrane proteins, including integrins (yellow), sarcoglycans (purple), and  $\beta$ -dystroglycan (green).  $\beta$ -dystroglycan connects the sarcolemma with the extracellular matrix (ECM) via  $\alpha$ -dystroglycan. Dystrophin links the costamere to the cytoskeleton through its association with actin and  $\alpha$ -actinin via ankyrin-G and obscurin.

**C**, Confocal image of murine ventricular cardiomyocyte stained for Na<sub>v</sub>1.5 (red) and Bin1 (green), showing Na<sub>v</sub>1.5 expression at the intercalated disc, lateral membrane, and an intracellular punctate pattern coinciding with Bin1 signal. Scale bar 20  $\mu$ m.

By characterizing Na<sub>v</sub>1.5 organization and expression at different pools at a nanoscale and addressing their pool-specific determinants, we contribute to the understanding of pathophysiological variety in patients carrying *SCN5A* mutations, as mutations may affect Na<sub>v</sub>1.5 pools differently. The 2 genetic mouse models investigated in this study give insight into pool-specific effects of a Na<sub>v</sub>1.5 mutation ( $\Delta$ SIV) and of disturbing Na<sub>v</sub>1.5 regulation (*mdx*). It appears that (1) Na<sub>v</sub>1.5 is expressed in T-tubules; (2) dystrophin deficiency increases T-tubular Na<sub>v</sub>1.5 expression; (3) Na<sub>v</sub>1.5 expression is reduced at the lateral membrane of *mdx* and  $\Delta$ SIV mice overall, whereas groove expression is specifically reduced in  $\Delta$ SIV cells; and (4) Na<sub>v</sub>1.5 cluster organization changes at the lateral membrane of *mdx* cells and in T-tubules of *mdx* and  $\Delta$ SIV cells compared with wild type (WT).

## METHODS

For detailed methods, we refer to the Expanded methods. The data that support the findings of this study are available from the corresponding author upon request.

### Mouse Models

All animal experiments conformed to the Guide to the Care and Use of Laboratory Animals (US National Institutes of Health, Publication No. 85-23, revised 1996); were approved by the Cantonal Veterinary Administration, Bern, Switzerland; conformed to the New York University guidelines for animal use and care (IACUC Protocol 160726-03 to Dr Delmar, approved 07/11/2018); and have complied with the Swiss Federal Animal Protection Law.

The *mdx*<sup>5CV</sup> mouse strain displays total deletion of dystrophin protein and was generated as described previously.<sup>25</sup> In  $\Delta$ SIV knockin mice, the C-terminal SIV motif of Na<sub>v</sub>1.5 was deleted as described previously.<sup>5</sup>

### Isolation of Murine Ventricular Myocytes

Cardiomyocytes were isolated based on a previously established enzymatic method.<sup>8</sup>

### Microscopy Sample Preparation

Freshly isolated cardiomyocytes were stained with antibodies against Na<sub>v</sub>1.5, Bin1, and  $\alpha$ -actinin, and imaged on a confocal microscope or with SMLM.

### Single-Molecule Localization Microscopy

SMLM imaging, single-molecule localization, and image processing were performed according to a previously described method.<sup>26,27</sup> Image simulations were performed using the Interaction Factor plugin in ImageJ.<sup>28</sup>

### Detubulation

Isolated cardiomyocytes were detubulated using formamide based on a previously described method.<sup>29</sup>

## Electrophysiology

Whole-cell  $I_{Na}$  was recorded using  $\approx$ 2 M $\Omega$  borosilicate glass pipettes.

## Statistics

Data are presented as means $\pm$ SD. Differences between 2 groups were analyzed by 2-tailed *t* tests if the data were normally distributed, and Mann-Whitney *U* tests if the data were not. *P*<0.05 was considered statistically significant.

## RESULTS

### Na<sub>v</sub>1.5 Occurs at Distinct Pools in Murine Ventricular Cardiomyocytes

The main focus of this work is the characterization of Na<sub>v</sub>1.5 localization and cluster organization in different cardiomyocyte domains with novel quantitative SMLM and modeling. Technical validation of SMLM is shown in Figure 1 in the [Data Supplement](#). We first gained a general overview over the Na<sub>v</sub>1.5 pools with confocal microscopy. We immunostained isolated murine ventricular cardiomyocytes for Na<sub>v</sub>1.5 and the T-tubular marker Bin1. Na<sub>v</sub>1.5 is visible at the lateral membrane and intercalated disc (Figure 1C). Some Na<sub>v</sub>1.5 seems to colocalize with Bin1, the latter showing a striated pattern that indicates the T-tubular membrane. The limited resolution and sensitivity of the confocal microscope, however, prevents us from establishing a detailed quantitative analysis of Na<sub>v</sub>1.5 in the T-tubules (Figure 1C).

To determine the molecular characteristics of Na<sub>v</sub>1.5 expression at the lateral membrane by SMLM, we imaged the lateral membrane of WT cardiomyocytes stained for Na<sub>v</sub>1.5 and  $\alpha$ -actinin, which coincides with the groove (N=3, n=24; Figure 2A). Na<sub>v</sub>1.5 occurred both close to  $\alpha$ -actinin and in between  $\alpha$ -actinin clusters, indicating the groove and the crest, respectively (Figure 1A and 2A). To quantify whether the Na<sub>v</sub>1.5 clusters have an affinity for the groove, we used a novel analysis approach<sup>28</sup> based on Monte Carlo simulations in which Na<sub>v</sub>1.5 clusters were redistributed over the SMLM images (N=3, n=24) either randomly or with a high affinity for  $\alpha$ -actinin (Figure 2B and 2C). For high-affinity simulations, an interaction factor (IF) of 0.7 was assumed, given that IF=0.0 represents random overlap between the 2 colors, IF=1.0 perfect overlap, and IF $\geq$ 0.5 indicates that a color has significant affinity for the other.<sup>28</sup> Then, for the original and simulated images, the edge distance from each  $\alpha$ -actinin cluster to the closest Na<sub>v</sub>1.5 cluster was determined. Na<sub>v</sub>1.5 clusters within 50 nm from  $\alpha$ -actinin were considered to be expressed in the groove. Twenty-three percent of Na<sub>v</sub>1.5 clusters were in the groove in experimental images. This value approached that of the simulations with high affinity for  $\alpha$ -actinin (25%; Figure 2D). In random simulations, only 15% of Na<sub>v</sub>1.5 clusters were

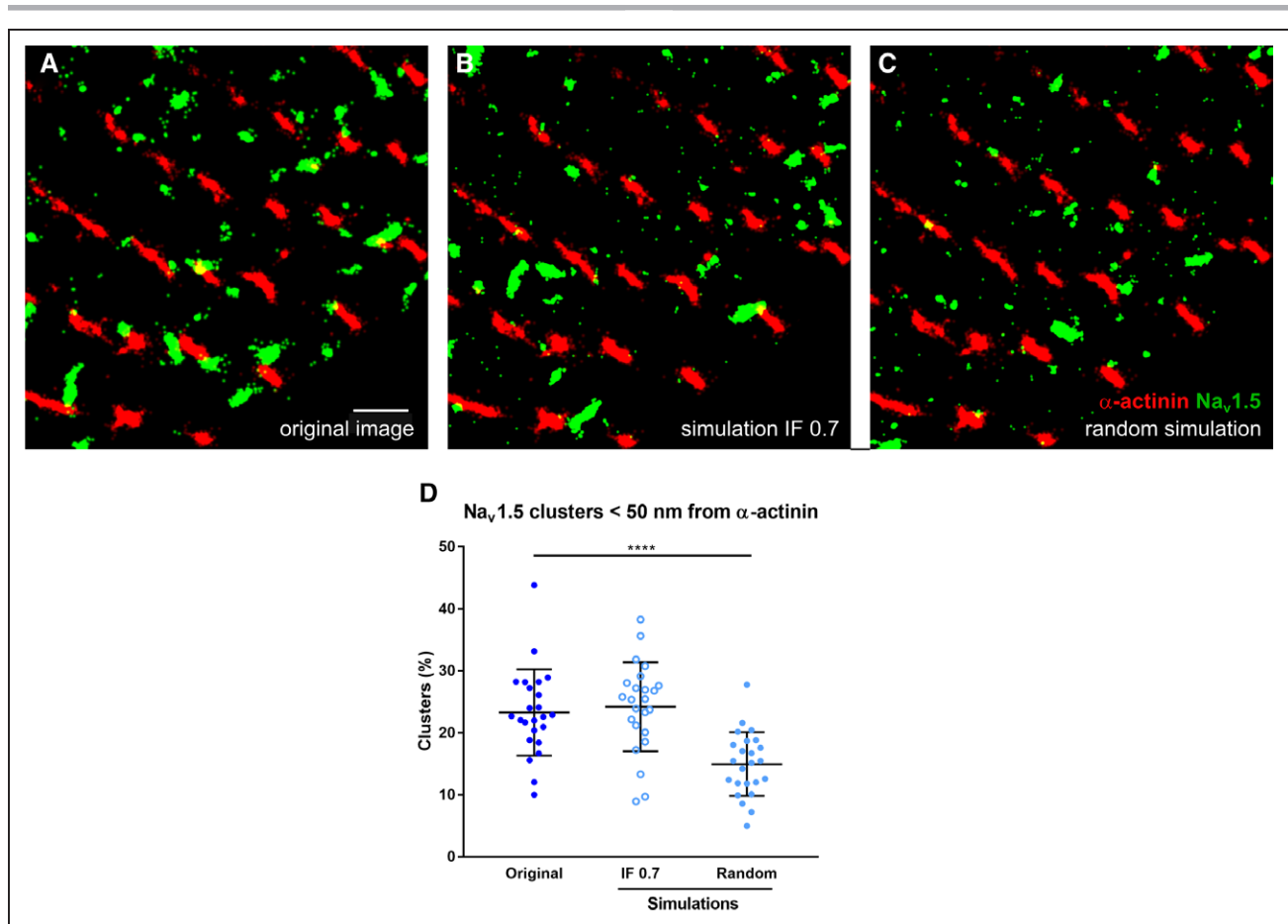


**Figure 2. The cardiac voltage-gated sodium channel Na<sub>v</sub>1.5 has affinity for the groove at the lateral membrane of a cardiomyocyte.** **A**, Super-resolution image of the lateral membrane of murine ventricular myocyte stained for Na<sub>v</sub>1.5 (green) and  $\alpha$ -actinin (red). Na<sub>v</sub>1.5 occurs close to  $\alpha$ -actinin, indicating the groove, and in between  $\alpha$ -actinin lines, indicating the crest. Scale bar 1  $\mu$ m. Na<sub>v</sub>1.5 clusters of the single-molecule localization microscopy (SMLM) images (**A**) were redistributed randomly (**B**) or with a high affinity for  $\alpha$ -actinin (interaction factor [IF] 0.7 [**C**]). Note that differences in affinity cannot be identified by eye in the small area given here. **D**, In original SMLM images of wild-type (WT) cells (N=3, n=24), the proportion of Na<sub>v</sub>1.5 within 50 nm of  $\alpha$ -actinin is  $\approx$ 30% higher than in simulations in which Na<sub>v</sub>1.5 clusters are distributed randomly. \*\*\*\* $P < 0.0001$ , Mann-Whitney *U* test.

within 50 nm from  $\alpha$ -actinin. These results strongly suggest that Na<sub>v</sub>1.5 has an affinity for the groove.

### Na<sub>v</sub>1.5 Expression at the Lateral Membrane and the Groove Depends on Dystrophin and the $\Delta$ SIV Motif, Whereas Cluster Organization Depends on Dystrophin Only

Our SMLM-derived metrics indicate that Na<sub>v</sub>1.5 cluster density at the lateral membrane is reduced by  $\approx$ 30% in *mdx* and  $\Delta$ SIV cardiomyocytes compared with WT cells (Figure 3A through 3D; WT N=3, n=24; *mdx* N=3, n=27;  $\Delta$ SIV N=3, n=19). These observations accord with previously reported results<sup>57</sup> and confirm the specificity of the anti-Na<sub>v</sub>1.5 antibody. Cell and average Na<sub>v</sub>1.5 cluster size did not change between genotypes, although *mdx* cells showed a high variability in Na<sub>v</sub>1.5 cluster size (Figure IIA in the Data Supplement). Na<sub>v</sub>1.5 cluster solidity and circularity were markedly higher in *mdx* cells compared

with WT (Figure IIA in the Data Supplement). Given that solidity is defined as the ratio between the particle area and the convex hull area of the particle, and circularity as the roundness of a particle (1.0 indicating a perfect circle), the increased solidity and circularity indicate that Na<sub>v</sub>1.5 clusters have geometrically less complex shapes.

To assess the effects of Na<sub>v</sub>1.5 truncation and dystrophin deficiency on Na<sub>v</sub>1.5 expression at the groove, we compared the distances from each  $\alpha$ -actinin cluster to the closest Na<sub>v</sub>1.5 cluster between *mdx*,  $\Delta$ SIV, and WT lateral membrane images. The frequency histogram (Figure 3E) shows that the proportion of Na<sub>v</sub>1.5 clusters within 50 nm of  $\alpha$ -actinin is reduced by  $\approx$ 25% in *mdx* and  $\Delta$ SIV compared with WT cells. Considering the proportion of Na<sub>v</sub>1.5 within 50 nm of  $\alpha$ -actinin for each individual cell (Figure 3F),  $\Delta$ SIV cardiomyocytes show a significant  $\approx$ 20% reduction compared with WT. Although mean Na<sub>v</sub>1.5 expression in *mdx* cells is reduced by  $\approx$ 17% compared with WT, the data show high variability (Figure 3F), which correlates with the high variability

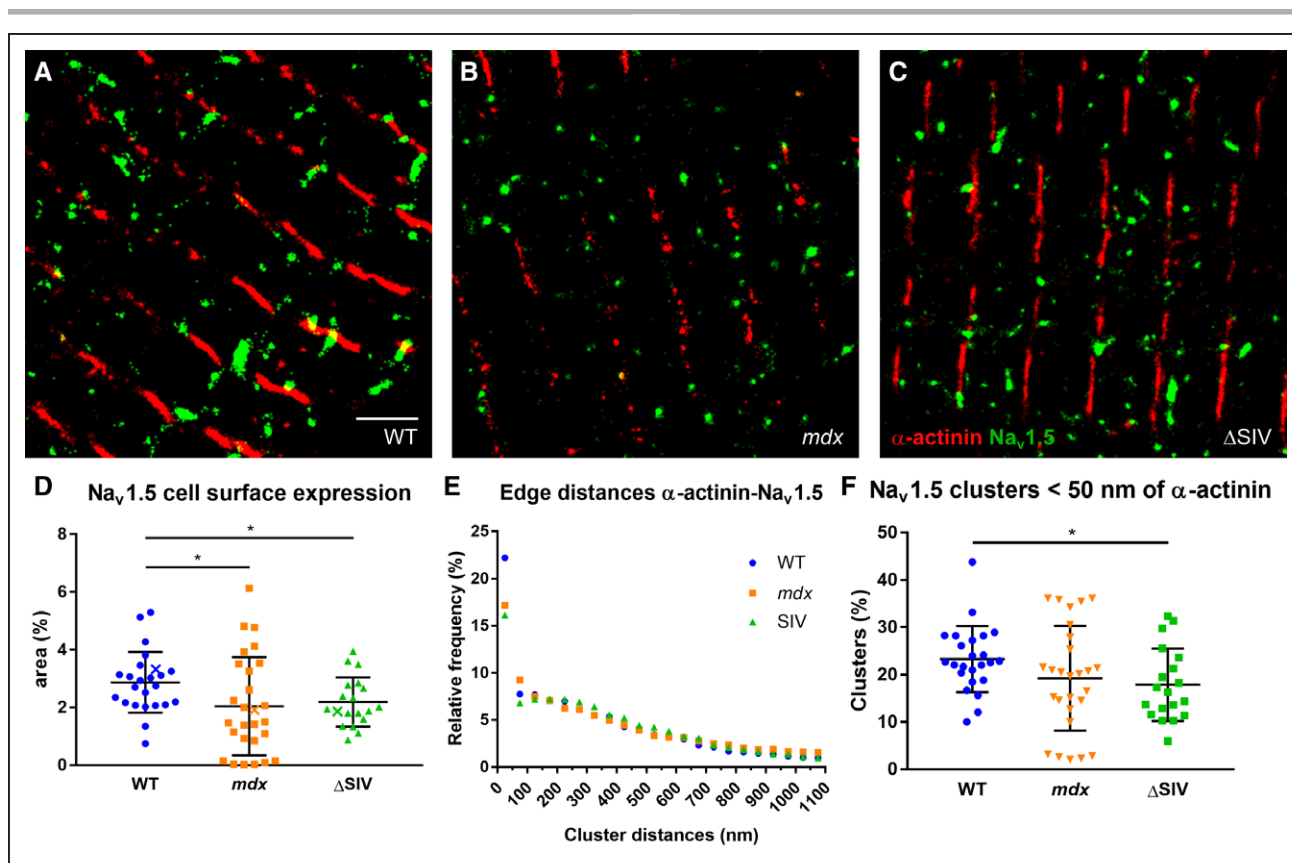


**Figure 3.** ΔSIV and dystrophin-deficient (*mdx*) cardiomyocytes show loss of the cardiac voltage-gated sodium channel Na<sub>v</sub>1.5 expression at the lateral membrane.

**A–C,** Detail of single-molecule localization microscopy (SMLM) images of the lateral membrane from wild type (WT; **A**), *mdx* (**B**), and ΔSIV (**C**) cells. Scale bar 1.5 μm. **D,** Total Na<sub>v</sub>1.5 expression at the lateral membrane is reduced by ≈30% in *mdx* and ΔSIV compared with WT. Data points represented by a cross (x) correspond to examples from **A–C**. **E,** Frequency distribution plot of edge distances from any α-actinin cluster to the closest Na<sub>v</sub>1.5 cluster. Bin (bridging integrator) size 50 nm. **F,** Groove expression of Na<sub>v</sub>1.5, defined as Na<sub>v</sub>1.5 clusters within 50 nm of Bin1, is reduced by ≈30% in ΔSIV cardiomyocytes compared with WT. WT N=3, n=24; *mdx* N=3, n=27; and ΔSIV N=3, n=19. \**P*=0.024 (WT vs *mdx* [**D**]); *P*=0.016 (WT vs ΔSIV [**D**]); *P*=0.019 (WT vs ΔSIV [**F**]), Mann-Whitney *U* test.

in Na<sub>v</sub>1.5 expression at the lateral membrane of *mdx* cells (Figure 3D). The affinity of Na<sub>v</sub>1.5 for the groove is similar in WT, *mdx*, and ΔSIV cells when comparing the proportion of Na<sub>v</sub>1.5 clusters within 50 nm of α-actinin from experimental images with random and high-affinity simulations for each genotype (Figure IIIA in the [Data Supplement](#)).

These results establish that (1) Na<sub>v</sub>1.5 expression at the groove of the lateral membrane partially depends on the SIV motif and dystrophin; (2) in dystrophin-deficient cells, Na<sub>v</sub>1.5 clusters at the lateral membrane organize into simpler shapes compared with WT cells; and (3) dystrophin deficiency induces high variability in Na<sub>v</sub>1.5 expression and cluster size.

### Na<sub>v</sub>1.5 Is Expressed in the T-Tubular Membrane

The T-tubular Na<sub>v</sub>1.5 expression was assessed by imaging intracellular planes of cardiomyocytes stained for Na<sub>v</sub>1.5 and the T-tubular marker Bin1. Bin1 is a solid T-tubular marker since it binds and shapes the T-tubular

membrane.<sup>30</sup> The Bin1 antibody was validated by confirming that Bin1 signals are in close proximity to α-actinin, given that T-tubules run in close proximity to the sarcomeric Z-disc (N=3, n=59; Figure IV in the [Data Supplement](#)).<sup>24</sup> We assessed whether Na<sub>v</sub>1.5 and Bin1 associated randomly or not by performing simulations for each SMLM image (N=3, n=39) where Na<sub>v</sub>1.5 clusters were redistributed randomly, or with high (IF 0.7) affinity for Bin1 (Figure 4A through 4C). In addition, we included borderline affinity simulations (IF 0.5), since this IF value is the lowest to indicate protein-protein interactions. The frequency histogram (Figure 4D) shows that about 15% to 17% of Na<sub>v</sub>1.5 clusters are within 50 nm of Bin1 in both original images and high-affinity simulations but only ≈8% in random simulations. We observed a similar pattern when plotting for each image the proportion of Na<sub>v</sub>1.5 clusters within 50 nm of Bin1 (Figure 4E). We found that the proportion of Na<sub>v</sub>1.5 clusters within 50 nm from Bin1 is 26% higher in original images than in borderline affinity simulations (Figure 4E). These findings

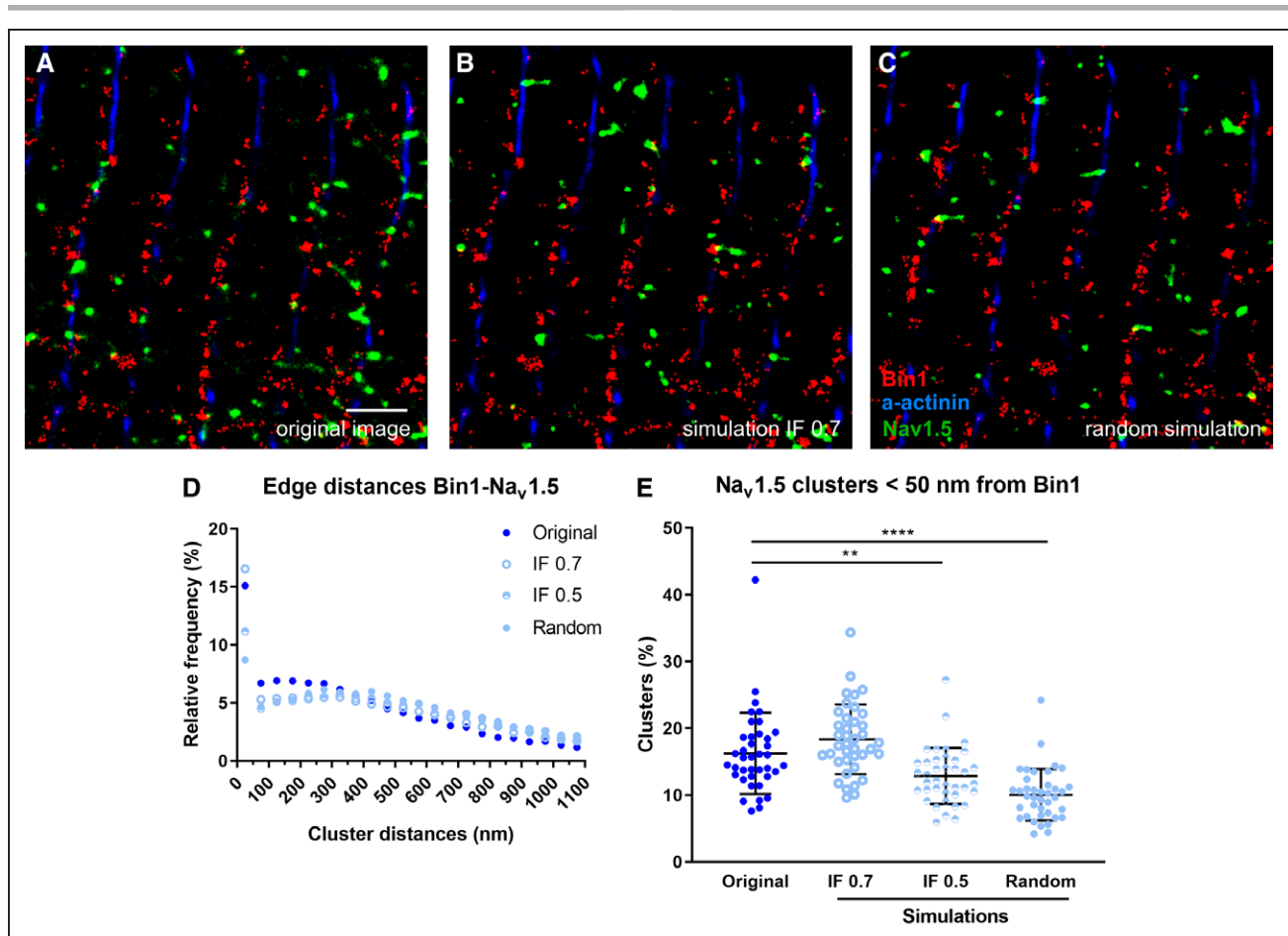


**Figure 4. The cardiac voltage-gated sodium channel Na<sub>v</sub>1.5 is expressed in the T-tubules.**

**A**, Detail of an intracellular recording from a wild-type (WT) cardiomyocyte stained for Na<sub>v</sub>1.5 (green), Bin1 (bridging integrator 1; red), and α-actinin (blue). All Na<sub>v</sub>1.5 clusters are redistributed over the image randomly (**B**), with high affinity for Bin1 (interaction factor [IF] 0.7 [**C**]), or with borderline affinity for Bin1 (IF 0.5; not shown). Scale bar 1.5 μm. **D**, Frequency distribution of distances from each Bin1 to the closest Na<sub>v</sub>1.5 cluster (N=3, n=39). **E**, In experimental single-molecule localization microscopy (SMLM) images, a higher proportion of Na<sub>v</sub>1.5 is within 50 nm from the nearest Bin1 than in random (+60%) or borderline affinity simulations (+26%), but not as much as in simulations with a high-affinity simulations (IF 0.7; -11%). Values for each individual cell/simulation are plotted. \*\*\*\*P<0.0001, unpaired *t* test.

indicate that a sizeable subset of intracellular Na<sub>v</sub>1.5 is expressed in the T-tubular membrane.

### T-Tubular I<sub>Na</sub> Cannot Be Assessed by Whole-Cell Recordings

Having shown that Na<sub>v</sub>1.5 is expressed at the T-tubules (Figure 4), we investigated whether we could record a T-tubular I<sub>Na</sub>. We compared whole-cell I<sub>Na</sub> recordings from normal (N=5, n=7) and detubulated (N=5, n=7) ventricular cardiomyocytes. Detubulation was successful as the capacitance of detubulated cells was 30% lower than of control cells (Figure 5B). Whole-cell I<sub>Na</sub> did not decrease after detubulation (Figure 5A) indicating that sodium channels at the intercalated disc and lateral membrane conduct the vast majority of I<sub>Na</sub>. Current densities show a 25% yet nonsignificant I<sub>Na</sub> density increase after detubulation (Figure 5C), confirming that the majority of sodium channels are outside the

T-tubular domain. Current densities, however, cannot be compared directly as capacitance measurements in control cardiomyocytes result in a considerable underestimation of cell membrane area.<sup>16</sup> Thus, the T-tubular I<sub>Na</sub> is below the detection limit of the whole-cell patch-clamp technique.

### Na<sub>v</sub>1.5 Expression Is Increased in T-Tubules From Dystrophin-Deficient Cardiomyocytes, and Cluster Organization Depends on the SIV Motif and Dystrophin

We next investigated whether dystrophin deficiency and SIV motif deletion affected Na<sub>v</sub>1.5 expression in the T-tubules. Overall Na<sub>v</sub>1.5 cluster density in intracellular planes was higher in *mdx* compared with WT cells, whereas no difference was observed between ΔSIV and WT cells (Figure 6A; WT N=3, n=47; *mdx* N=3, n=26; ΔSIV N=3, n=13). Compared with WT cells, cluster

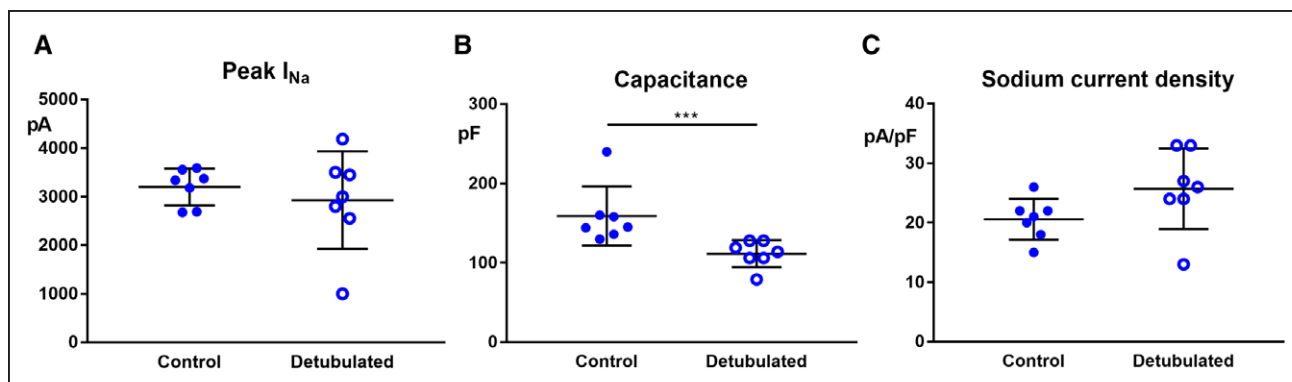


**Figure 5. Whole-cell sodium current recordings in detubulated and normal cardiomyocytes.**

Compared with control cells, maximum sodium current (**A**) did not change, capacitance (**B**) was reduced by  $\approx 30\%$ , and sodium current density (**C**) increased nonsignificantly in detubulated cells.  $N=5$ ,  $n=7$  for both conditions.  $***P=0.006$ , Mann-Whitney test.

solidity in *mdx* and circularity in *mdx* and  $\Delta$ SIV were increased, while cell size and average Na<sub>v</sub>1.5 cluster size did not differ (Figure II in the [Data Supplement](#)). Similar to the lateral membrane, intracellular Na<sub>v</sub>1.5 clusters have geometrically simpler shapes in intracellular planes of *mdx* and  $\Delta$ SIV cells.

The frequency histogram for Bin1-Na<sub>v</sub>1.5 edge distances shows that the proportion of Na<sub>v</sub>1.5 within 50 nm to Bin1 was  $\approx 30\%$  higher in *mdx* and  $\approx 4\%$  higher in  $\Delta$ SIV compared with WT (Figure 6B; WT  $N=3$ ,  $n=39$ ; *mdx*  $N=3$ ,  $n=20$ ;  $\Delta$ SIV  $N=3$ ,  $n=11$ ). Plotting these values from individual cells confirmed the increase of T-tubular Na<sub>v</sub>1.5 in *mdx* cells, but no difference between  $\Delta$ SIV and WT cells was observed (Figure 6C). When comparing T-tubular Na<sub>v</sub>1.5 expression from original images with random, borderline affinity and high-affinity simulations, Na<sub>v</sub>1.5 displays considerable affinity for Bin1 in all 3 genotypes (Figure IIIB in the [Data Supplement](#)).

These data indicate that dystrophin deficiency but not SIV deletion induces a higher Na<sub>v</sub>1.5 expression associated with intracellular membrane compartments and T-tubules. Intracellular Na<sub>v</sub>1.5 cluster shapes were moreover simpler in  $\Delta$ SIV and *mdx* compared with WT cardiomyocytes.

## DISCUSSION

This work aimed to surpass the previously published limited-resolution characterization of Na<sub>v</sub>1.5 expression and cluster organization at the lateral membrane and T-tubules of cardiomyocytes. To this end, we applied novel quantitative SMLM and modeling techniques to investigate Na<sub>v</sub>1.5 organization at the lateral membrane and T-tubules in cardiomyocytes from WT mice, *mdx* mice, and mice expressing C-terminally truncated Na<sub>v</sub>1.5 ( $\Delta$ SIV). We showed that (1) Na<sub>v</sub>1.5 expression in the lateral membrane groove partly depends on dystrophin

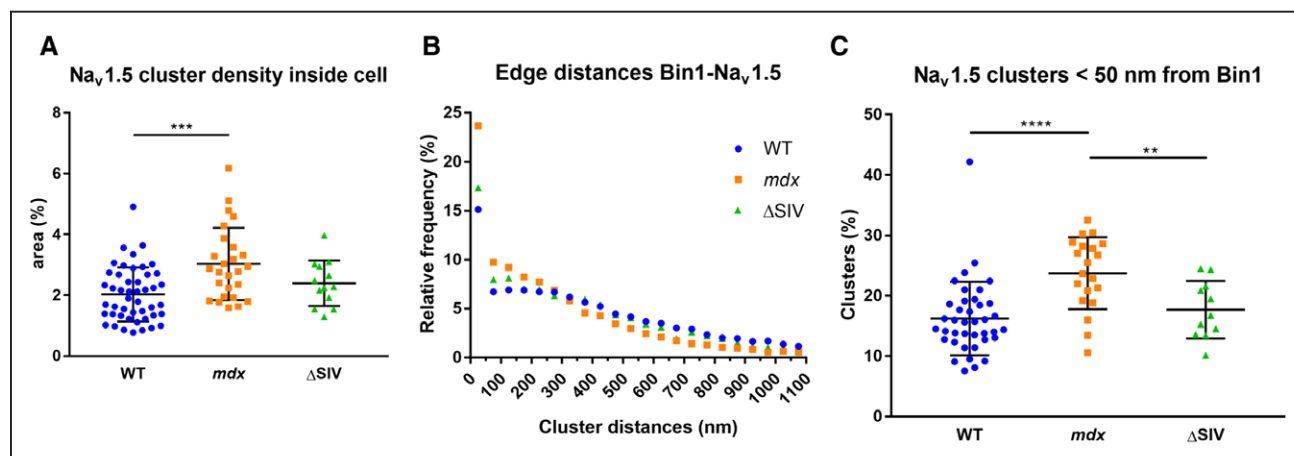


**Figure 6. The cardiac voltage-gated sodium channel Na<sub>v</sub>1.5 expression is increased in T-tubules of dystrophin-deficient (*mdx*) mice.**

**A**, Na<sub>v</sub>1.5 cluster density in intracellular membrane compartments and T-tubules is  $\approx 30\%$  higher in *mdx* cardiomyocytes than in wild-type (WT) cardiomyocytes. **B**, For each Bin1 (bridging integrator 1) cluster, distances to the closest Na<sub>v</sub>1.5 cluster were measured and plotted in a frequency histogram with bins of 50 nm. **C**, In *mdx* cells, a higher proportion of Na<sub>v</sub>1.5 clusters is within 50 nm from Bin1 than in WT cells.  $\Delta$ SIV cells show a similar T-tubular Na<sub>v</sub>1.5 expression as WT cells. **A**, WT  $N=3$ ,  $n=47$ ; *mdx*  $N=3$ ,  $n=26$ ;  $\Delta$ SIV  $N=3$ ,  $n=13$ . **B** and **C**, WT  $N=3$ ,  $n=39$ ; *mdx*  $N=3$ ,  $n=20$ ;  $\Delta$ SIV  $N=3$ ,  $n=11$ .  $**P=0.0095$ ;  $***P=0.0002$ ;  $****P<0.0001$ , Mann-Whitney *U* test.

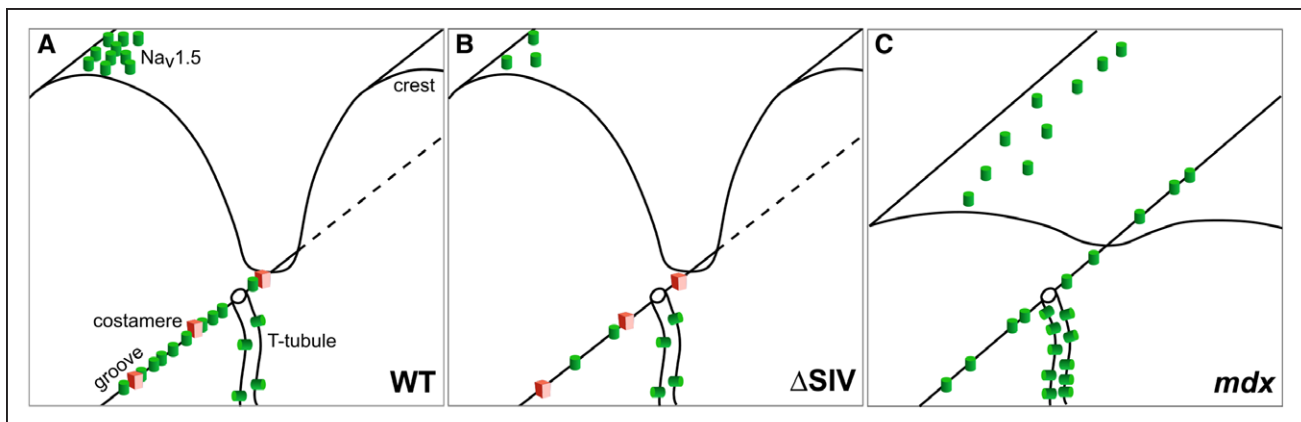


**Figure 7. Model depicting changes at the lateral membrane and T-tubules of  $\Delta$ SIV and dystrophin-deficient (*mdx*) cardiomyocytes.**

Compared with wild type (WT; **A**),  $\Delta$ SIV cells (**B**) show less cardiac voltage-gated sodium channels Na<sub>v</sub>1.5 at the lateral membrane overall and specifically in the groove, whereas lateral membrane structure remains intact. In *mdx* cells (**C**), the lateral membrane flattened, and Na<sub>v</sub>1.5 expression at the lateral membrane is reduced overall; yet the expression at groove of *mdx* cells is not as affected as that of  $\Delta$ SIV cells. Costameres are severely compromised in *mdx* cells. In the T-tubules, Na<sub>v</sub>1.5 expression is similar in WT (**A**) and  $\Delta$ SIV cells (**B**), and increased in *mdx* cardiomyocytes (**C**).

and the Na<sub>v</sub>1.5 SIV motif; (2) dystrophin is involved in Na<sub>v</sub>1.5 cluster organization at the lateral membrane; (3) Na<sub>v</sub>1.5 is expressed in the T-tubules; (4) T-tubular Na<sub>v</sub>1.5 expression is increased in dystrophin-deficient but not in  $\Delta$ SIV cardiomyocytes; and (5) intracellular Na<sub>v</sub>1.5 cluster organization depends on dystrophin and SIV (Figure 7).

We convincingly showed that Na<sub>v</sub>1.5 is expressed in the T-tubules by costaining Na<sub>v</sub>1.5 with the T-tubular marker Bin1 in SMLM recordings and assessing the robustness of this association by novel in silico methods.<sup>27,28</sup> Comparing original images to simulations in which Na<sub>v</sub>1.5 clusters were redistributed randomly or with high affinity for Bin1, we observed that the T-tubular population of Na<sub>v</sub>1.5 in original images is twice as high as in random populations and comparable to that in high-affinity simulations (Figure 4E). The function of Na<sub>v</sub>1.5 at the T-tubules remains elusive, although Na<sub>v</sub>1.5 in the T-tubules will theoretically increase conduction velocity.<sup>6</sup> Since some Bin1 and Na<sub>v</sub>1.5 clusters overlapped (Figure 4A), we hypothesize that Bin1 may regulate Na<sub>v</sub>1.5 in the T-tubules as Bin1 regulates trafficking of the L-type voltage-gated calcium channel.<sup>31</sup>

The presence of a T-tubular  $I_{Na}$  could not be deduced from whole-cell electrophysiological methods as currents from detubulated and control cardiomyocytes were similar (Figure 5A). T-tubular  $I_{Na}$  may not surpass the noise of whole-cell recordings, or the T-tubular membrane may not be properly voltage-clamped in our whole-cell approach (space clamp issue), thus a proportion of T-tubular sodium channels may not activate. Brette et al<sup>15</sup> have suggested that the T-tubular  $I_{Na}$  is  $\approx 30\%$  of total  $I_{Na}$  by comparing current densities from detubulated and control cells. Measuring capacitance in control cardiomyocytes underestimates cell membrane area, however, disqualifying the direct comparison of current

densities from nondetubulated and detubulated cells.<sup>16</sup> Other electrophysiological methods could not record T-tubular currents either: cell-attached<sup>21</sup> and scanning ion conductance microscopy data<sup>11,20</sup> show currents from only a few voltage-gated calcium channels where a much stronger calcium current would be expected. To assess the T-tubular  $I_{Na}$ , more specific methods need to be developed.

When dystrophin is absent, less Na<sub>v</sub>1.5 is expressed at the lateral membrane (Figure 3A), while more Na<sub>v</sub>1.5 is expressed in the T-tubules compared with WT cells (Figure 6C). The reduction Na<sub>v</sub>1.5 at the lateral membrane of *mdx* cells may be related to the loss of costamere integrity (Figure 7).<sup>32</sup> Na<sub>v</sub>1.5 trafficking may be partly rerouted to the T-tubules. The short dystrophin product Dp71 may be involved since it is present only at the T-tubules<sup>33</sup> and binds ion channels.<sup>34</sup> Given the overall reduction in Na<sub>v</sub>1.5 protein expression and  $I_{Na}$  in *mdx* hearts,<sup>8</sup> the relative increase of T-tubular Na<sub>v</sub>1.5 expression may make matters worse: due to the restricted space in the T-tubular lumen, a larger T-tubular  $I_{Na}$  may partly self-attenuate,<sup>35,36</sup> which may have a net slowing effect on macroscopic conduction. This effect may contribute to the reduction in ventricular conduction velocity observed in *mdx* mice.<sup>6,8</sup>

Na<sub>v</sub>1.5 cluster shapes in the groove and the intracellular compartment are simpler in *mdx* than in WT cells (Figure II in the [Data Supplement](#)). This indicates that dystrophin may shape Na<sub>v</sub>1.5 clusters, which may be related to the large size (427 kD) of dystrophin, and to the link to the actin cytoskeleton that dystrophin provides.<sup>37</sup> In  $\Delta$ SIV cells, Na<sub>v</sub>1.5 clusters show an increase in solidity in intracellular planes only (Figure IIB in the [Data Supplement](#)). Thus, at the lateral membrane, the secondary N-terminal syntrophin-binding site of Na<sub>v</sub>1.5<sup>38</sup> may

support interaction with dystrophin and WT-like Na<sub>v</sub>1.5 cluster organization.

The dystrophin homologue utrophin may explain the residual Na<sub>v</sub>1.5 expression at the lateral membrane of *mdx* mice.<sup>39</sup> Utrophin is expressed during the fetal phase and re-expressed in adult tissue when dystrophin is absent in mice, but not in humans.<sup>39,40</sup> The high variability in Na<sub>v</sub>1.5 cluster density and size at the lateral membrane and at the groove in *mdx* cells (Figure 3A and 3C, Figure IIA in the [Data Supplement](#)) may be caused by different levels in compensatory utrophin and Dp71 expression. Utrophin, however, does not rescue a WT-like phenotype, and the crest-groove profile at the lateral membrane of *mdx* cardiomyocytes is flattened compared with WT (Figure 7C).<sup>41</sup> The effects of dystrophin deficiency when the aforementioned compensatory mechanisms are not available need to be assessed in heart samples from Duchenne patients and from dystrophin/utrophin/Dp71 knockout mice.

Like *mdx* mice,  $\Delta$ SIV mice express less Na<sub>v</sub>1.5 at the lateral membrane, and the groove pool is specifically affected (Figure 3D and 3F).  $\Delta$ SIV truncation reduces the interaction of Na<sub>v</sub>1.5 with the syntrophin-dystrophin complex<sup>5</sup>; therefore, the syntrophin-dystrophin complex may play a role in Na<sub>v</sub>1.5 stability and forward trafficking. Since  $\Delta$ SIV mice express dystrophin, costameres presumably remain intact. Of note, the syntrophin-dystrophin complex may also interact with the N-terminus of Na<sub>v</sub>1.5,<sup>38</sup> possibly explaining part of the residual Na<sub>v</sub>1.5 expression at the groove and the lateral membrane. Moreover, part of the lateral membrane population of Na<sub>v</sub>1.5 seems to be syntrophin-independent, as shown in syntrophin knockout mice.<sup>21</sup> Contrary to *mdx* mice, we did not observe an increase of Na<sub>v</sub>1.5 at the T-tubules in  $\Delta$ SIV mice, which may be explained by their intact costameres.

Although some domain-specific interaction partners of Na<sub>v</sub>1.5 are known (such as connexin-43 at the intercalated disc<sup>42</sup> and syntrophin and CASK at the lateral membrane<sup>8,9</sup>), we expect that many molecular determinants of Na<sub>v</sub>1.5 at the crest, groove, and T-tubules remain to be identified. These interaction partners may affect Na<sub>v</sub>1.5 trafficking (like connexin-43<sup>42</sup>), stability (like syntrophin<sup>8</sup>), and  $I_{Na}$  properties (like syntrophin and CASK<sup>8,9</sup>) and will provide a toolbox for Na<sub>v</sub>1.5 fine-tuning in a location-specific manner.

A groove-specific reduction of Na<sub>v</sub>1.5, as shown for  $\Delta$ SIV and a subset of *mdx* cardiomyocytes, and an increase in T-tubular Na<sub>v</sub>1.5, as shown for *mdx* cells, may affect conduction and excitability in different ways. However, late openings between the crest and the groove as well as biophysical properties did not differ in murine cardiomyocytes.<sup>11</sup> We hypothesize that a reduction in groove Na<sub>v</sub>1.5 does not slow longitudinal conduction per se as charge very quickly redistributes over the cell.<sup>43</sup> An overall reduction in Na<sub>v</sub>1.5, however, will slow conduction. Alternatively, a recent study suggests that lateral

membranes from adjacent cardiomyocytes can be close together.<sup>10</sup> If the lateral membranes are close enough to support ephaptic conduction,<sup>44–46</sup> the specific localization of lateral membrane Na<sub>v</sub>1.5 may prove crucial. Ephaptic conduction is mediated by electric fields and is yet mainly explored at the intercalated disc.<sup>44–46</sup> Future studies should address specific differences in function and regulation of Na<sub>v</sub>1.5 in the crest, groove, and T-tubules.

Intriguingly, while our data revealed that Na<sub>v</sub>1.5 is reduced at the groove of *mdx* and  $\Delta$ SIV mice, Rivaud et al<sup>11</sup> have recently shown in a murine heart failure model that  $I_{Na}$  is reduced at the crest, not at the groove, compared with sham-operated animals. Rivaud et al showed that Na<sub>v</sub>1.5 cluster size, not cluster density, was reduced at the lateral membrane in the heart failure model, whereas our data show that cluster density, not cluster size, was reduced in *mdx* and  $\Delta$ SIV cells (Figure IIA in the [Data Supplement](#)). Expression and organization of Na<sub>v</sub>1.5 at the crest and the groove was not investigated in this heart failure model. Together, these data suggest that cardiomyocytes respond differently to dystrophin deficiency, Na<sub>v</sub>1.5 truncation ( $\Delta$ SIV), and heart failure.<sup>11</sup> One obvious difference is the hypertrophy observed in the heart failure model but not in *mdx* or  $\Delta$ SIV mice. The different underlying pathways remain to be elucidated.

Like  $\Delta$ SIV cardiomyocytes, cardiomyocytes from Brugada syndrome patients carrying the mutation p.V2016M, which changes the C-terminal motif SIV into SIM, may show a reduction in Na<sub>v</sub>1.5 cluster density in the lateral membrane groove, dystrophin-Na<sub>v</sub>1.5 interaction,<sup>8</sup> and intracellular cluster complexity. Such modifications may contribute to the Brugada syndrome phenotype. Indeed, in  $\Delta$ SIV cardiomyocytes, transversal conduction velocity, total  $I_{Na}$ , and  $I_{Na}$  at the lateral membrane are decreased.<sup>5</sup> Future research should characterize Na<sub>v</sub>1.5 cluster organization and subcellular expression patterns in cardiomyocytes from mouse models and humans expressing channelopathy-associated Na<sub>v</sub>1.5 mutations. Moreover, new techniques need to be developed to correlate conduction in tissue (loading cells with voltage dyes with millisecond resolution) with the (re)distribution of channels in this tissue on SMLM scale. Alternatively, an elaborate in silico finite-element model of cardiac cells could explore the relationship between channel distribution and anisotropy.

A limitation of our study is that the small sample size and variance in some of the measures limit the potential significance of the findings. *mdx* mice moreover display various compensatory mechanisms discussed above that do not allow us to assess the effects of a pure dystrophin deficiency. In addition, *mdx* mice do not have the optimal controls, since they were on a Bl6/Ros background while being backcrossed to Bl/6J in the fourth generation, whereas WT and  $\Delta$ SIV mice were littermates on a pure Bl6/J background. The discrepancy in backgrounds may have introduced variability in our data, although the

data are consistent with previously published results.<sup>7B</sup> Last, our methods did not allow us to quantify crest expression of Na<sub>v</sub>1.5.

Taken together, our findings provide important and previously unattainable mechanistic insights on the properties of Na<sub>v</sub>1.5 organization on the crest, groove, and lateral membrane of cardiomyocytes and are an important step towards identifying cardiac domain-specific molecular determinants of Na<sub>v</sub>1.5 and location-specific effects of *SCN5A* mutations. However, pool-specific function and regulation of Na<sub>v</sub>1.5 at the crest, groove, and T-tubules remain to be studied in more detail.

## ARTICLE INFORMATION

Received December 9, 2019; accepted May 6, 2020.

### Affiliations

Institute of Biochemistry and Molecular Medicine, University of Bern, Switzerland (S.H.V., J.-S.R., H.A.). Microscopy Core, Icahn School of Medicine at Mount Sinai, New York, NY (E.A.-P.). Department of Biochemistry and Pharmacology (E.R.) and Department of Cardiology (M.D.), New York University School of Medicine, NY.

### Acknowledgments

We express our gratitude to Marta Pérez-Hernández Durán, Alejandra Leo-Macias, and Yandong Yin (NYUMC), and to Maria Essers and Sabrina Guichard (University of Bern) for their stellar technical assistance. We thank Sarah Keegan (NYUMC) for providing the Python scripts.

### Sources of Funding

Drs Abriel and Vermij acknowledge funding from the Swiss National Science Foundation (grant no. 310030\_165741 [Dr Abriel] and P1BEP3\_172237 [Dr Vermij]).

### Disclosures

None.

## REFERENCES

- Gellens ME, George AL Jr, Chen LQ, Chahine M, Horn R, Barchi RL, Kallen RG. Primary structure and functional expression of the human cardiac tetrodotoxin-insensitive voltage-dependent sodium channel. *Proc Natl Acad Sci U S A*. 1992;89:554–558. doi: 10.1073/pnas.89.2.554
- Veerman CC, Wilde AA, Lodder EM. The cardiac sodium channel gene *SCN5A* and its gene product Nav1.5: role in physiology and pathophysiology. *Gene*. 2015;573:177–187. doi: 10.1016/j.gene.2015.08.062
- Wilde AAM, Amin AS. Clinical spectrum of *SCN5A* mutations: long qt syndrome, brugada syndrome, and cardiomyopathy. *JACC Clin Electrophysiol*. 2018;4:569–579. doi: 10.1016/j.jacep.2018.03.006
- Vermij SH, Abriel H, van Veen TA. Refining the molecular organization of the cardiac intercalated disc. *Cardiovasc Res*. 2017;113:259–275. doi: 10.1093/cvr/cvw259
- Shy D, Gillet L, Ogrodnik J, Albesa M, Verkerk AO, Wolswinkel R, Rougier JS, Barc J, Essers MC, Syam N, et al. PDZ domain-binding motif regulates cardiomyocyte compartment-specific Nav1.5 channel expression and function. *Circulation*. 2014;130:147–160. doi: 10.1161/CIRCRESAHA.113.007852
- Vermij SH, Abriel H, Kucera JP. A fundamental evaluation of the electrical properties and function of cardiac transverse tubules. *Biochim Biophys Acta Mol Cell Res*. 2020;1867:118502. doi: 10.1016/j.bbamcr.2019.06.016
- Petitprez S, Zmoos AF, Ogrodnik J, Balse E, Raad N, El-Haou S, Albesa M, Bittihn P, Luther S, Lehnart SE, et al. SAP97 and dystrophin macromolecular complexes determine two pools of cardiac sodium channels Nav1.5 in cardiomyocytes. *Circ Res*. 2011;108:294–304. doi: 10.1161/CIRCRESAHA.110.228312
- Gavillet B, Rougier JS, Domenighetti AA, Behar R, Boixel C, Ruchat P, Lehr HA, Pedrazzini T, Abriel H. Cardiac sodium channel Nav1.5 is regulated by a multiprotein complex composed of syntrophins and dystrophin. *Circ Res*. 2006;99:407–414. doi: 10.1161/01.RES.0000237466.13252.5e
- Eichel CA, Beuriot A, Chevalier MY, Rougier JS, Louault F, Dilanian G, Amour J, Coulombe A, Abriel H, Hatem SN, et al. Lateral membrane-specific MAGUK CASK down-regulates Nav1.5 channel in cardiac myocytes. *Circ Res*. 2016;119:544–556. doi: 10.1161/CIRCRESAHA.116.309254
- Guilbeau-Frugier C, Cauquil M, Karsenty C, Lairez O, Dambrin C, Payré B, Cassard H, Josse C, Seguelas MH, Allart S, et al. Structural evidence for a new elaborate 3D-organization of the cardiomyocyte lateral membrane in adult mammalian cardiac tissues. *Cardiovasc Res*. 2019;115:1078–1091. doi: 10.1093/cvr/cvy256
- Rivaud MR, Agullo-Pascual E, Lin X, Leo-Macias A, Zhang M, Rothenberg E, Bezzina CR, Delmar M, Remme CA. Sodium channel remodeling in subcellular microdomains of murine failing cardiomyocytes. *J Am Heart Assoc*. 2017;6:e007622. doi: 10.1161/JAHA.117.007622
- Bhargava A, Lin X, Novak P, Mehta K, Korchev Y, Delmar M, Gorelik J. Super-resolution scanning patch clamp reveals clustering of functional ion channels in adult ventricular myocyte. *Circ Res*. 2013;112:1112–1120. doi: 10.1161/CIRCRESAHA.111.300445
- Bootman MD, Higazi DR, Coombes S, Roderick HL. Calcium signalling during excitation-contraction coupling in mammalian atrial myocytes. *J Cell Sci*. 2006;119(pt 19):3915–3925. doi: 10.1242/jcs.03223
- Kawai M, Hussain M, Orchard CH. Excitation-contraction coupling in rat ventricular myocytes after formamide-induced detubulation. *Am J Physiol*. 1999;277:H603–H609. doi: 10.1152/ajpheart.1999.277.2.H603
- Brette F, Orchard CH. Density and sub-cellular distribution of cardiac and neuronal sodium channel isoforms in rat ventricular myocytes. *Biochem Biophys Res Commun*. 2006;348:1163–1166. doi: 10.1016/j.bbrc.2006.07.189
- Pásek M, Brette F, Nelson A, Pearce C, Qaiser A, Christie G, Orchard CH. Quantification of t-tubule area and protein distribution in rat cardiac ventricular myocytes. *Prog Biophys Mol Biol*. 2008;96:244–257. doi: 10.1016/j.pbiomolbio.2007.07.016
- Mohler PJ, Rivolta I, Napolitano C, LeMaillet G, Lambert S, Priori SG, Bennett V. Nav1.5 E1053K mutation causing brugada syndrome blocks binding to ankyrin-G and expression of Nav1.5 on the surface of cardiomyocytes. *Proc Natl Acad Sci U S A*. 2004;101:17533–17538. doi: 10.1073/pnas.0403711101
- Ponce-Balbuena D, Guerrero-Serna G, Valdivia CR, Caballero R, Diez-Guerra FJ, Jiménez-Vázquez EN, Ramírez RJ, Monteiro da Rocha A, Herron TJ, Campbell KF, et al. Cardiac Kir2.1 and Nav1.5 channels traffic together to the sarcolemma to control excitability. *Circ Res*. 2018;122:1501–1516. doi: 10.1161/CIRCRESAHA.117.311872
- Lin X, Liu N, Lu J, Zhang J, Anumonwo JM, Isom LL, Fishman GI, Delmar M. Subcellular heterogeneity of sodium current properties in adult cardiac ventricular myocytes. *Heart Rhythm*. 2011;8:1923–1930. doi: 10.1016/j.hrthm.2011.07.016
- Lab MJ, Bhargava A, Wright PT, Gorelik J. The scanning ion conductance microscope for cellular physiology. *Am J Physiol Heart Circ Physiol*. 2013;304:H1–11. doi: 10.1152/ajpheart.00499.2012
- Rougier JS, Essers MC, Gillet L, Guichard S, Sonntag S, Shmerling D, Abriel H. A distinct pool of Nav1.5 channels at the lateral membrane of murine ventricular cardiomyocytes. *Front Physiol*. 2019;10:834. doi: 10.3389/fphys.2019.00834
- Domínguez JN, de la Rosa A, Navarro F, Franco D, Aránega AE. Tissue distribution and subcellular localization of the cardiac sodium channel during mouse heart development. *Cardiovasc Res*. 2008;78:45–52. doi: 10.1093/cvr/cvm118
- Yin Y, Lee WTC, Rothenberg E. Ultrafast data mining of molecular assemblies in multiplexed high-density super-resolution images. *Nat Commun*. 2019;10:119. doi: 10.1038/s41467-018-08048-2
- Fu Y, Hong T. BIN1 regulates dynamic t-tubule membrane. *Biochim Biophys Acta*. 2016;1863(7 Pt B):1839–1847. doi: 10.1016/j.bbamcr.2015.11.004
- Chapman VM, Miller DR, Armstrong D, Caskey CT. Recovery of induced mutations for X chromosome-linked muscular dystrophy in mice. *Proc Natl Acad Sci U S A*. 1989;86:1292–1296. doi: 10.1073/pnas.86.4.1292
- Yin Y, Lee WTC, Rothenberg E. Ultrafast data mining of molecular assemblies in multiplexed high-density super-resolution images. *Nat Commun*. 2019;10:119. doi: 10.1038/s41467-018-08048-2
- Leo-Macias A, Agullo-Pascual E, Sanchez-Alonso JL, Keegan S, Lin X, Arcos T, Feng-Xia-Liang, Korchev YE, Gorelik J, Fenyő D, et al. Nanoscale visualization of functional adhesion/excitability nodes at the intercalated disc. *Nat Commun*. 2016;7:10342. doi: 10.1038/ncomms10342

28. Bermudez-Hernandez K, Keegan S, Whelan DR, Reid DA, Zagelbaum J, Yin Y, Ma S, Rothenberg E, Fenyö D. A method for quantifying molecular interactions using stochastic modelling and super-resolution microscopy. *Sci Rep*. 2017;7:14882. doi: 10.1038/s41598-017-14922-8
29. Brette F, Komukai K, Orchard CH. Validation of formamide as a detubulation agent in isolated rat cardiac cells. *Am J Physiol Heart Circ Physiol*. 2002;283:H1720–H1728. doi: 10.1152/ajpheart.00347.2002
30. Hong T, Yang H, Zhang SS, Cho HC, Kalashnikova M, Sun B, Zhang H, Bhargava A, Grabe M, Olgin J, et al. Cardiac BIN1 folds T-tubule membrane, controlling ion flux and limiting arrhythmia. *Nat Med*. 2014;20:624–632. doi: 10.1038/nm.3543
31. Hong TT, Smyth JW, Gao D, Chu KY, Vogan JM, Fong TS, Jensen BC, Colecraft HM, Shaw RM. BIN1 localizes the L-type calcium channel to cardiac T-tubules. *PLoS Biol*. 2010;8:e1000312. doi: 10.1371/journal.pbio.1000312
32. Bonuccelli G, Sotgia F, Schubert W, Park DS, Frank PG, Woodman SE, Insabato L, Cammer M, Minetti C, Lisanti MP. Proteasome inhibitor (MG-132) treatment of mdx mice rescues the expression and membrane localization of dystrophin and dystrophin-associated proteins. *Am J Pathol*. 2003;163:1663–1675. doi: 10.1016/S0002-9440(10)63523-7
33. Masubuchi N, Shidoh Y, Kondo S, Takatoh J, Hanaoka K. Subcellular localization of dystrophin isoforms in cardiomyocytes and phenotypic analysis of dystrophin-deficient mice reveal cardiac myopathy is predominantly caused by a deficiency in full-length dystrophin. *Exp Anim*. 2013;62:211–217. doi: 10.1538/expanim.62.211
34. Hernández-González EO, Mornet D, Rendon A, Martínez-Rojas D. Absence of Dp71 in mdx3cv mouse spermatozoa alters flagellar morphology and the distribution of ion channels and nNOS. *J Cell Sci*. 2005;118(pt 1):137–145. doi: 10.1242/jcs.01584
35. Hatano A, Okada J, Washio T, Hisada T, Sugiura S. An integrated finite element simulation of cardiomyocyte function based on triphasic theory. *Front Physiol*. 2015;6:287. doi: 10.3389/fphys.2015.00287
36. Vermij SH, Abriel H, Kucera JP. Modeling depolarization delay, sodium currents, and electrical potentials in cardiac transverse tubules. *Front Physiol*. 2019;10:1487. doi: 10.3389/fphys.2019.01487
37. Amann KJ, Renley BA, Ervasti JM. A cluster of basic repeats in the dystrophin rod domain binds F-actin through an electrostatic interaction. *J Biol Chem*. 1998;273:28419–28423. doi: 10.1074/jbc.273.43.28419
38. Matamoros M, Pérez-Hernández M, Guerrero-Serna G, Amorós I, Barana A, Núñez M, Ponce-Balbuena D, Sacristán S, Gómez R, Tamargo J, et al. Nav1.5 N-terminal domain binding to  $\alpha$ 1-syntrophin increases membrane density of human Kir2.1, Kir2.2 and Nav1.5 channels. *Cardiovasc Res*. 2016;110:279–290. doi: 10.1093/cvr/cvv009
39. Albesa M, Ogradnik J, Rougier JS, Abriel H. Regulation of the cardiac sodium channel Nav1.5 by utrophin in dystrophin-deficient mice. *Cardiovasc Res*. 2011;89:320–328. doi: 10.1093/cvr/cvq326
40. Liao HK, Hatanaka F, Araoka T, Reddy P, Wu MZ, Sui Y, Yamauchi T, Sakurai M, O'Keefe DD, Núñez-Delgado E, et al. *In Vivo* target gene activation via CRISPR/Cas9-mediated trans-epigenetic modulation. *Cell*. 2017;171:1495–1507.e15. doi: 10.1016/j.cell.2017.10.025
41. Lorin C, Gueffier M, Bois P, Faivre JF, Cognard C, Sebille S. Ultrastructural and functional alterations of EC coupling elements in mdx cardiomyocytes: an analysis from membrane surface to depth. *Cell Biochem Biophys*. 2013;66:723–736. doi: 10.1007/s12013-013-9517-8
42. Agullo-Pascual E, Lin X, Leo-Macias A, Zhang M, Liang FX, Li Z, Pfenninger A, Lübke-meier I, Keegan S, Fenyö D, et al. Super-resolution imaging reveals that loss of the C-terminus of connexin43 limits microtubule plus-end capture and Nav1.5 localization at the intercalated disc. *Cardiovasc Res*. 2014;104:371–381. doi: 10.1093/cvr/cvu195
43. Krassowska W, Neu JC. Response of a single cell to an external electric field. *Biophys J*. 1994;66:1768–1776. doi: 10.1016/S0006-3495(94)80971-3
44. Kucera JP, Rohr S, Rudy Y. Localization of sodium channels in intercalated disks modulates cardiac conduction. *Circ Res*. 2002;91:1176–1182. doi: 10.1161/01.res.0000046237.54156.0a
45. Hichri E, Abriel H, Kucera JP. Distribution of cardiac sodium channels in clusters potentiates ephaptic interactions in the intercalated disc. *J Physiol*. 2018;596:563–589. doi: 10.1113/JP275351
46. Rhett JM, Veeraraghavan R, Poelzing S, Gourdie RG. The perinexus: signpost on the path to a new model of cardiac conduction? *Trends Cardiovasc Med*. 2013;23:222–228. doi: 10.1016/j.tcm.2012.12.005